Analysis of Hand Contact Areas and Interaction Capabilities During Manipulation and Exploration

Franck Gonzalez, *Student Member, IEEE*, Florian Gosselin, and Wael Bachta

Abstract—Manual human-computer interfaces for virtual reality are designed to allow an operator interacting with a computer simulation as naturally as possible. Dexterous haptic interfaces are the best suited for this goal. They give intuitive and efficient control on the environment with haptic and tactile feedback. This paper is aimed at helping in the choice of the interaction areas to be taken into account in the design of such interfaces. The literature dealing with hand interactions is first reviewed in order to point out the contact areas involved in exploration and manipulation tasks. Their frequencies of use are then extracted from existing recordings. The results are gathered in an original graphical interaction map allowing for a simple visualization of the way the hand is used, and compared with a map of mechanoreceptors densities. Then an interaction tree, mapping the relative amount of actions made available through the use of a given contact area, is built and correlated with the losses of hand function induced by amputations. A rating of some existing haptic interfaces and guidelines for their design are finally achieved to illustrate a possible use of the developed graphical tools.

Index Terms—Human factors, ergonomics, human computer interactions, haptic interfaces, taxonomy

1 Introduction

The hand is a unique and versatile instrument allowing humans to interact intuitively and efficiently with their environment. For remote interaction, Shimoga argued that the telepresence and manipulation capabilities of an operator are enhanced by involving a dexterous master and a slave manipulator which end-effector mimics human hands [1]. Indeed, reproducing the interaction forces applied on the fingers increases the feeling of manipulating objects directly in the remote environment. Going beyond this line of reasoning would result in proposing haptic interfaces that could provide force feedback to the whole hand or to any part of its surface according to the ongoing manipulation task. However, this statement challenges the current mechanical design technologies. Thus in practice, a trade-off is usually made between design simplicity and interaction capabilities.

Most existing haptic interfaces make use of tool-mediated interactions. In this case, the design is simplified but the user's dexterity is limited and only a subset of tasks can be reproduced. A wider set of activities can be addressed with dexterous haptic devices. However practically, in order to keep such systems within an acceptable level of complexity and bulk, the number of considered contact areas between the haptic interface and the hand of the operator is decreased. This results in a small number of robotized fingers and less Degrees Of Freedom (DOF) per finger. The addressed contact areas are usually chosen with respect to the targeted task. In [2], it has been argued that two-finger interfaces addressing the index and thumb are sufficient to deal with fine manipulation of small objects in an educational context. In [3], the authors analyzed interactions within a car cockpit and concluded that a three-finger haptic interface addressing the thumb, the index, and the middle fingertips is necessary to render such interactions in a proper way. Another approach is proposed in [4]. An encounter-type device is designed to physically replicate the geometry of some empirically selected objects. However it may not reflect the contact surfaces involved in general interactions.

To go beyond such task-dependent approaches, this paper intends a general answer which may be of interest for the design of any dexterous system. It intends to provide some tools to help in the selection of the appropriate contact areas as a function of manipulation capabilities and design complexity.

In Section 2, a review of several grasp taxonomies [5], [6] and exploratory ones [7] allows to define contact areas on the hand surface. These areas are weighted by their frequencies of use according to data extracted from [8]. First, the results are merged into graphical hand interaction maps highlighting the use of the glabrous skin areas for usual manipulation and exploration tasks. Then, these maps are compared to the location of the mechanoreceptors. In Section 3, various combinations of the contact areas are sorted in a graphical interaction tree, providing an insight on the relative amount of possible interactions as a function of the number of considered contact areas. The obtained result is then correlated to the lost hand function due to amputations. In Section 4 a classification of several existing haptic interfaces and some guidelines for their design illustrate a

- *F. Gonzalez is with the CEA, LIST, Interactive Robotics Laboratory, F-91190 Gif-sur-Yvette, France, and Sorbonne Universités, UPMC Univ Paris 06, CNRS UMR 7222, INSERM U 1150, Institut des Systèmes Intelligents et de Robotique, Equipe Agathe, F-75005 Paris, France. E-mail: franck.gonzalez@cea.fr.*
- *F. Gosselin is with the CEA, LIST, Interactive Robotics Laboratory, F-91190 Gif-sur-Yvette, France. E-mail: florian.gosselin@cea.fr.*
- *W. Bachta is with Sorbonne Universités, UPMC Univ Paris 06, CNRS UMR 7222, INSERM U 1150, Institut des Systèmes Intelligents et de Robotique, Equipe Agathe, F-75005 Paris, France. E-mail: wael.bachta@isir.upmc.fr.*

Manuscript received 17 June 2013; revised 9 Apr. 2014; accepted 18 Apr. 2014. Date of publication 1 May 2014; date of current version 15 Dec. 2014. Recommended for acceptance by A. Okamura.
For information on obtaining reprints of this article, please send e-mail to: reprints@ieee.org, and reference the Digital Object Identifier below.
Digital Object Identifier no. 10.1109/TOH.2014.2321395

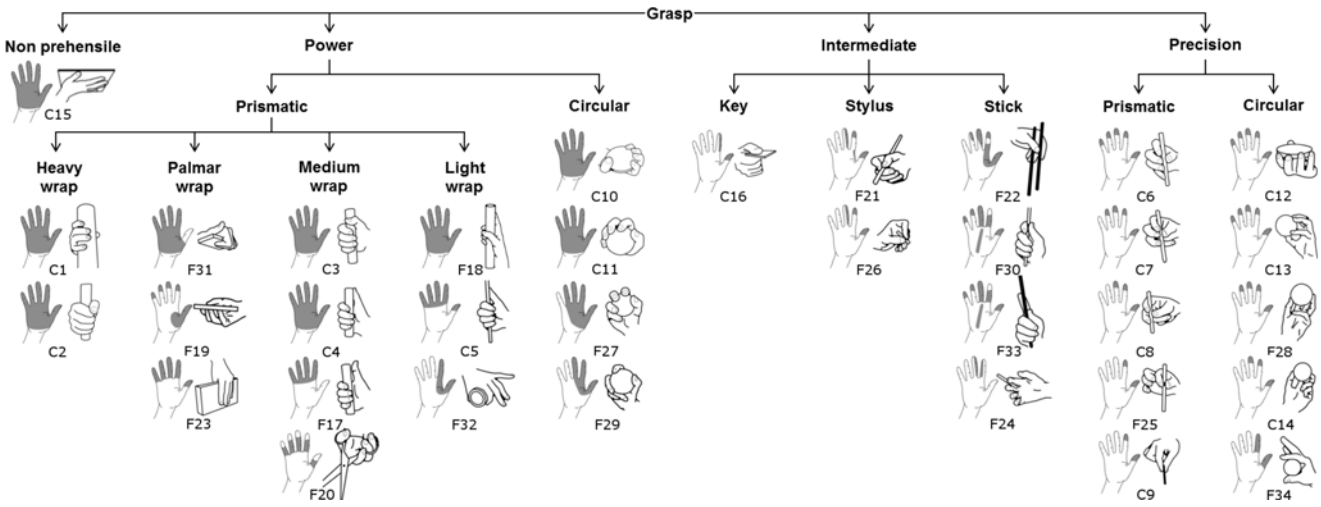

Fig. 1. A comprehensive grasp taxonomy and the corresponding contact surfaces.

use of this interaction tree. Finally, Section 5 discusses some possible further developments.

2 Analysis of Hand Interaction Areas: Building a Hand Interaction Map

Any hand interaction with the environment requires a contact that may be performed either to involve some changes, i.e., manipulation, and/or to gain some knowledge about its state, i.e., exploration. Both tasks will be investigated in the sequel.

2.1 Manipulation

The study of human grasping has been of interest in many research fields, resulting in a comprehensive literature in physiology and ergonomics [9], [10], [11]. In this field, the work of Cutkosky constitutes one of the major references in human grasping and is widely used for robotic and prosthetic hands designs [5]. He proposed a taxonomy which depicts 16 different patterns using task dexterity and precision as discriminants. However, some grasps are missing, e.g., holding a pen, and in everyday life numerous variations on the grasps are adopted depending on the context (sizes of the hand and object, personal preferences). Feix et al. proposed a more complete classification which includes *intermediate grasps* and is designed with respect to the posture of the hand [6]. Human manipulation behaviors can be further described by taking into account the hand's or object's motion, especially within hand as proposed by Bullock et al. [12]. However, as their categorization is less detailed for prehensile patterns, in this work we chose to merge the taxonomy of Cutkosky, taken as the basis, with the grasp types of Feix et al. which add a finer level of distinction (Fig. 1). Each pattern is called $C_{i\in[\![1,16]\!]}$ or $F_{j\in[\![17,34]\!]}$ whether it is part of the Cutkosky or Feix et al. taxonomy respectively (the correspondences between labels and grasp names are displayed in Table 1). This classification is easily readable and provides a wide overview of grasping as it takes into account power, intermediate and precision grasps.

For each above pattern, the surface in contact with the hand is extracted (Fig. 1). It is chosen here to sort the tree vertically as an increasing function of the involved hand surface, i.e., from the bottom: use of only two fingertips, to the top: whole internal hand surface. Power grasps are displayed on the left and precision ones on the right, with intermediate grasps in the middle. Some previously highlighted characteristics of the taxonomies appear clearly, like the use of the fingertips only in precision patterns, the involvement of a lateral surface in most intermediate grasps, and the majority of the glabrous skin surface in power grasps. One can also note that the same contact surface can be used for different grasps, like for *thumb-4 finger* (C_6) and *precision sphere* (C_{13}), although the grasps differ on the geometry of the object being held. Except for Cutkosky's *platform push* (C_{15}), non-prehensile patterns are not included. One can note that other patterns could be easily integrated into the tree.

TABLE 1
A List of the Grasps Considered in This Article, from [5] and Feix et al.'s Database (*grasp.xief.net*)

Non Prehensile & Power				Intermediate		Precision	
Label	Grasp	Label	Grasp	Label	Grasp	Label	Grasp
C_1	Large Diameter	F_{19}	Extension Type	C_{16}	Lateral Pinch	C_6	Thumb-4 Finger
C_2	Small Diameter	F_{20}	Distal Type	F_{21}	Writing Tripod	C_7	Thumb-3 Finger
C_3	Medium Wrap	F_{23}	Parallel Extension	F_{22}	Tripod Variation	C_8	Thumb-2 Finger
C_4	Adducted Thumb	F_{27}	Sphere-4 Finger	F_{24}	Adduction Grip	C_9	Thumb-Index Finger
C_5	Light Tool	F_{29}	Sphere-3 Finger	F_{26}	Lateral Tripod	C_{12}	(Precision) Disk
C_{10}	(Power) Disk	F_{31}	Palmar	F_{30}	Stick	C_{13}	(Precision) Sphere
C_{11}	(Power) Sphere	F_{32}	Ring	F_{33}	Ventral	C_{14}	Tripod
C_{15}	Hook, Platform Push					F_{25}	Tip Pinch
F_{17}	Fixed Hook					F_{28}	Quadpod
F_{18}	Index Finger Extension					F_{34}	Inferior Pincer

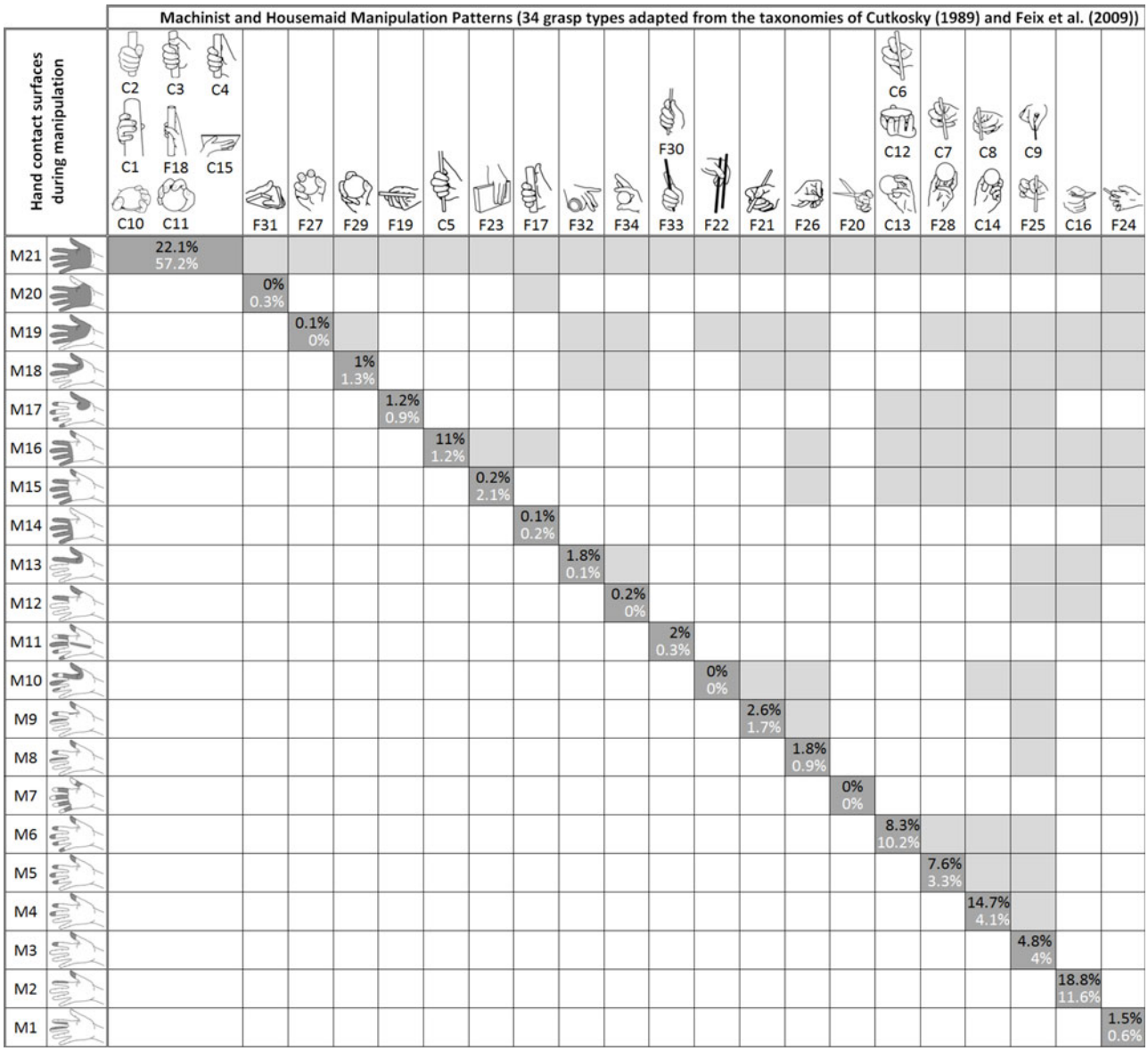

Fig. 2. A summary of available grasps in function of hand contact surfaces. The percentages correspond to the amount of time the hand contact surfaces are used during manipulation for a machinist (black) and a housemaid (white). In a given row, the light grey boxes highlight the hand contact surfaces that allow to perform a given column's grasp types.

The patterns and contact surfaces of Fig. 1 are reorganized and mapped together in Fig. 2. The hand areas involved in manipulation are sorted in the rows as an ascending function of their skin surface and labeled M_1 to M_{21}. As a whole, 21 contact surfaces are depicted, from the inner side of the index and middle fingers to the whole hand surface. The grasp patterns are given in columns. Those involving the same contact surfaces are grouped. They are connected through dark grey boxes: a given pattern (in the box's column) can be performed if a canonical contact surface (in the box's row) is involved. Conversely, a given contact surface allows to perform all its corresponding grasp types. These areas are inclusive, as highlighted with light grey boxes. For example, the five fingertips (M_6) grant access to the 5-fingered grasps (C_6, C_{12} and C_{13}), but also to any grasp made available through the use of 4 fingertips (C_7, F_{28}), 3 fingertips (C_8, C_{14}) and 2 fingertips (C_9, F_{25}). Similarly, the *sphere-three finger* (F_{29}) is performed provided that at least the thumb, index, middle and lateral side of the palm be involved, i.e., M_{18}, M_{19} and M_{21}. Of course, the whole hand (M_{21}) grants access to all 34 grasp types.

This scheme shows that the number of available grasps increases with the contact surface. However, it does not give any insight into the relative importance of each surface or grasp pattern, which can be defined as the time of use of a given grasp type over the total manipulation time (i.e., its frequency of use). Little information is available about the frequencies of use of the different grasp types in everyday life. In [9], a repartition of use is given (out of six defined patterns) showing that a *lateral tripod* (F_{26}, called "palmar" grasp) predominates over *thumb-index finger* and *lateral pinch* (C_9 and C_{16} respectively). This actually accounts for the design of common artificial hands [9] and matches the intuition but is insufficiently detailed. In a recent study, Zheng et al. designed an experimental procedure in order to record and analyze one's activities in an everyday situation over an

important amount of time [8]. They gave examples of a housemaid and a machinist, whose grasps have been recorded and sorted using the Cutkosky taxonomy first. The patterns that did not find a match in this classification have then been sorted according to Feix et al. The amount of time a pattern is used over the total grasping time is also provided. We chose to cross this information with the characteristic contact surfaces of Fig. 1 to compute the amount of time $T_{\%M_j}$ a contact surface M_j is used while performing a set of tasks, using the equation:

$$T_{\%M_j} = \sum_k T_{\%(C_k \text{ or } F_k)}, \quad (1)$$

with $T_{\%(C_k \text{ or } F_k)}$ the amount of time a grasp (C_k or F_k) involving M_j is used. The result is displayed in percentages in the dark grey boxes of Fig. 2 for both examples provided by Zheng et al.: in black for a machinist, in white for a housemaid. For instance, the five fingertips (M_6) are utilized in $8.3\% = 6\%(C_6) + 1.5\%(C_{12}) + 0.8\%(C_{13})$ of a given amount of time of usual activities of a machinist, whereas this ratio is $10.2\% = 3.1\%(C_6) + 0.4\%(C_{12}) + 6.7\%(C_{13})$ for a housemaid. A comparison of the percentages of the two examples shows a clear difference on the use of the contact surfaces, in correlation with the differences in the utilized grasp patterns. The housemaid uses more power grasps. This implies here a preponderance of tasks involving the whole hand. The contact surfaces corresponding to the "precision" branch of Fig. 1 are thus less highlighted in comparison with the machinist, for whom the balance between power and precision grasps accounts for a wider distribution. Furthermore, in both cases, the contact surface (M_2) corresponding to the *lateral pinch* (C_{16}), already mentioned by [9] as being of interest, is the second most utilized surface even if it refers to only one grasp.

These results take all their sense once cumulated on graphical interaction maps (Fig. 3, left). We divided the internal part of the hand in elementary interaction areas A_i by superimposing the boundaries of all contact surfaces. The cumulative frequency of use $T_{\%_c A_i}$ of an elementary hand area A_i is given by the following equation ($j \backslash A_i \subset M_j$ means that the frequency of use of a given contact surface M_j is accounted for a given area A_i only if A_i is included in M_j):

$$T_{\%_c A_i} = \sum_{j \backslash A_i \subset M_j} T_{\%M_j}, \quad (2)$$

and displayed in grayscale. One can note that some areas are of similar frequencies of use: in particular, the palm involves several areas which frequencies range from 22 to 28 percent for the machinist (from 58 to 61 percent for the housemaid) with a difference of less than 3 percent between adjacent areas. We chose to gather these zones (Fig. 3, right). The same holds for the metacarpus's areas, which were merged together with a frequency range of $[33; 39 \text{ percent}]$ for the machinist ($[59; 63 \text{ percent}]$ for the housemaid). The hand is thus divided in 12 *simplified* interaction areas (SIAs) from which all interaction areas can be obtained; however some of them make use of a part of the palm and metacarpus only.

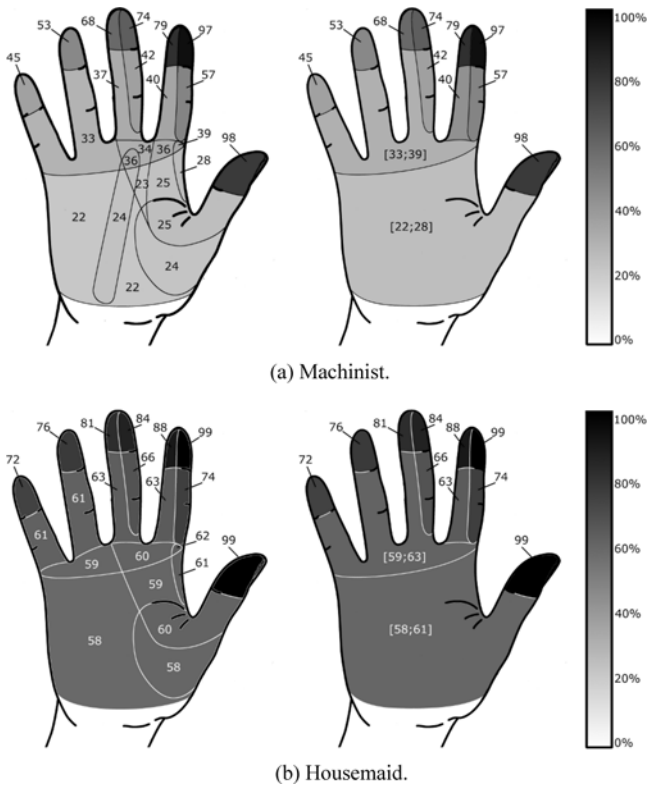

Fig. 3. Interaction maps for manipulation computed from equation (2) (left), and the corresponding simplified interaction areas (right). The frequencies of use (percent) are displayed both in grayscale and figures (examples from [8]).

The important information results more into the differences of contrast than in the level of grey itself as the data, although numerous enough to draw conclusions on a specific job, cannot constitute an average behavior over all types of human manipulation. Still, some similarities give a few directions. First, the fingertips are the privileged areas for manipulation, over the rest of the fingers and metacarpus (coming in second) and the palm and ulnar part of the hand. This meets the intuition and is within the conclusions of [9] and other researchers. This also accounts for the design of dexterous haptic interfaces that track movements and apply force feedback on the fingertips rather than on the rest of the hand.

As a second refinement, each fingertip does not have the same use. The thumb's intervenes 98 to 99 percent of the grasp time. The index's is the second most important, next comes the middle's. The ring's and little's are of lesser use. Finally, against the intuition, the index's external lateral surface attracts attention as it is used with the same frequency as the ring fingertip (albeit used in only one grasp: *lateral pinch* C_{16}). This may initiate a growing interest for this contact area.

2.2 Exploration

Researchers seem to agree that some stereotyped behaviors maintain some invariant properties during movements in order to evaluate the characteristics of a material [7]. They have been grouped in six exploratory procedures (Fig. 4, second row). Each one is optimal to a certain kind of information:

Hand contact surfaces during exploration		Exploration patterns (from Lederman and Klatzky (1987))				
		K3 K5	K4	K1	K2 K6	
E4		14.3%				
E3			9.5%			
E2				14.3%		
E1					61.9%	

Fig. 4. A summary of available exploratory procedures in function of the hand contact surfaces [7].

- *Lateral motion* (K_1) is used to gain knowledge about texture. Typically, the fingers rub across the surface.
- Hardness is sensed through *Pressure* (K_2). Normal forces are applied on the object, typically with the fingertip(s).
- A *Static contact* (K_3) allows to evaluate the temperature of an object. One hand rests on the object with a surface as large as possible, except in situations perceived as being possibly dangerous.
- The sense of weight is acquired through *Unsupported holding* (K_4). The object is held in a hand and moved using the arm or wrist.
- *Enclosure* (K_5) grants access to the global shape and volume of an object. The hand is in contact with as much of the envelope of the object as possible.
- The global and exact shape of an object can be sensed through *Contour following* (K_6). The hand moves while maintaining contact with the object.

The corresponding contact surfaces are extracted following the same framework as before and labelled E_1 to E_4 (some exploratory patterns share the same surfaces). The contact surfaces can vary in function of the object's size and shape. Furthermore in most cases, several information may be gathered simultaneously while manipulating an object, or a different finger may be involved. For example, it may be insecure to test an object's temperature with the whole hand like in drawing K_3 except if there is a prior knowledge on it. However, we chose to stick to Jones and Lederman's canonical objects.

The knowledge of the frequency of use of patterns K_1 to K_6 is necessary to quote the relative importance of the hand contact surfaces E_1 to E_4. This information can be indirectly found in [7], which provides data on precision, generality and duration of the six exploratory procedures. Each pattern is adapted to one property so none is prevailing. Thus it is assumed here that their frequency of use can be calculated as their duration over the needed time to perform all procedures (Fig. 4: K_1 (3 s), K_2 (2 s), K_3(<1 s), K_4 (2 s), K_5 (2 s), K_6 (11 s)).

These frequencies are gathered in the same way as for grasp types and displayed in the dark grey boxes of Fig. 4. As it is involved in several operations among which is the longest one (*contour following*), the index (E_1) is the most used whereas the centre of the hand (E_3), only used for the short duration *unsupported holding*, is less highlighted.

This data can be used to set up a hand interaction map for exploration. Like for manipulation, some elementary

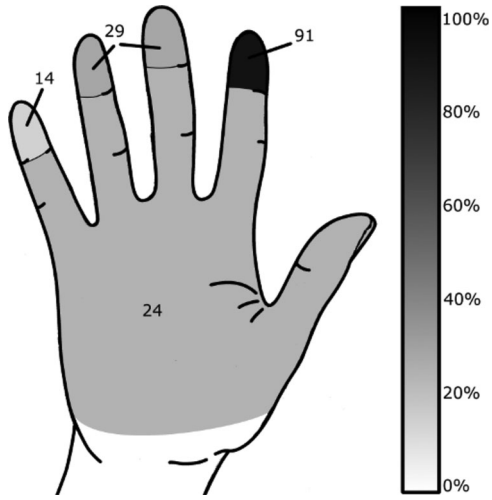

Fig. 5. Interaction map for manual exploration (percent).

contact areas are first defined by superimposing the boundaries from E_1 to E_4. Their cumulative frequencies of use are given by

$$T_{\%_c A_i} = \sum_{j \backslash A_i \subset E_j} T_{\%E_j}, \tag{3}$$

and displayed on Fig. 5. Here the distribution of the contact areas meets the intuition: the little is less involved than the rest of the hand while the index's fingertip is the most used.

2.3 General Hand Interaction Map

Considering that manual interactions involving contacts with the environment are mainly composed of exploration and manipulation, any interaction set is assumed to be characterized by a certain exploration/manipulation ratio. Moreover, the two interaction maps of Fig. 3 are thought to describe two different stereotypical manipulation behaviors: the housemaid mostly performs rough manipulation with power grasps and the machinist more delicate technical activities with both power and precision grasps. Therefore any average manipulation can be expressed as a ratio of these two maps. Consequently, any map of an interaction set may be approximated by a ratio between the three available maps in this article.

Fig. 6 displays the variations on the frequencies of use of the hand interaction areas in function of the ratio between two interaction maps (along the external bidirectional axes) or between the three interaction maps (centre). For this latter, an average behavior is compiled from the combination of the three maps with ratios varying from 25 to 50 percent. It can also be obtained by calculating a range of use for each interaction area taken separately and combining their frequencies of use for the machinist, housemaid and exploration with the same variation on ratios (e.g., M_4 is used 14.7, 4.1 and 0 percent of the time by resp. the machinist, housemaid and exploration. A mix of these values with ratios ranging from 25 to 50 percent causes the frequency of use of M_4 to be generally included in the range $[4.7; 8.4\ \text{percent}]$. The corresponding SIAs being the thumb, index (left and right

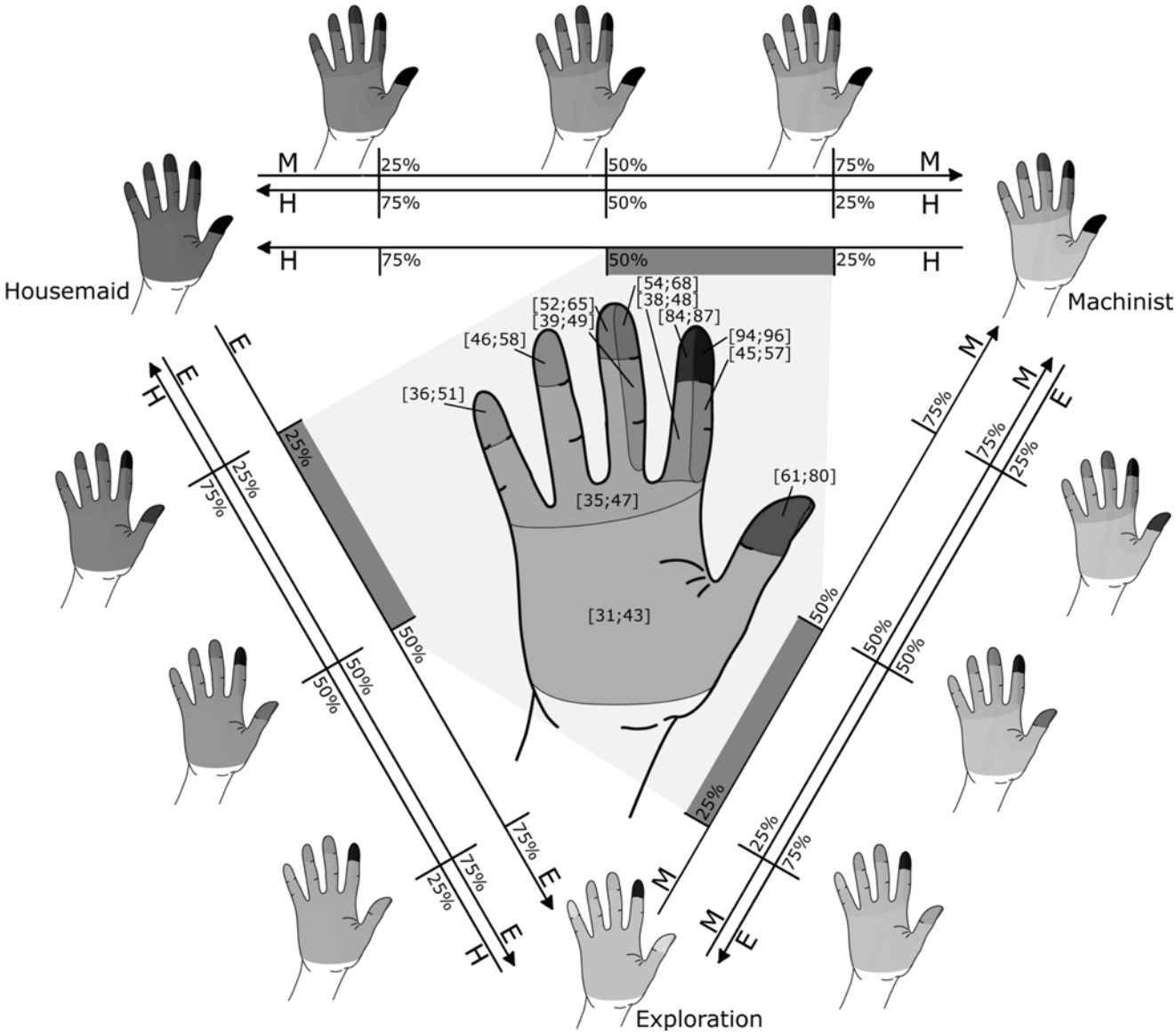

Fig. 6. Variations on the frequencies of use of the hand simplified interaction areas along the space defined by the three available maps of Figs. 3 and 5. Each external bidirectional axis refers to mixes of the two interaction maps at its ends, whereas the centre refers to a mix of the three interaction maps with weights ranging from 25 to 50 percent.

parts) and middle (left and right parts) fingertips, this range must be accounted for these five interaction areas and added to the contributions related to the other contact surfaces including those areas).

This general interaction map gives an overview on hand usage and shows coherent interaction behaviors. That is, the index fingertip is the most used, then comes the thumb's (although its frequency of use may vary more than for the rest of the fingertips), the middle's and the ring's (their variation is similar to the one of the index's external lateral surface). The little's fingertip appears to be used with the same frequency as the metacarpus. The palm is less used.

This data results from an ergonomic and behavioral methodology providing direct information on the most used hand areas. The next paragraph is aimed at correlating it with an indirect approach based on the examination of the density of the mechanoreceptors in the glabrous skin.

2.4 Sensorial System of the Glabrous Skin

The glabrous skin of the hand integrates a lot of mechanoreceptors which density can be assumed to reflect the importance of each surface in the sensorimotor process. That is, with respect to the role of each mechanoreceptor, a part with a higher density may be more utilized than another one. In the literature, four types of mechanoreceptors grant access to most of the available tactile data from the hand [13]:

A) FA I (fast adapting type I) afferents end in Meissner's corpuscles and respond to transient and high frequency deformations of the skin, important for edge contours and fine spatial details. They are the most numerous sensors.

B) SA I (slowly adapting type I) afferents end in Merkel's corpuscles. They are sensitive to low frequency dynamic skin deformations, static forces,

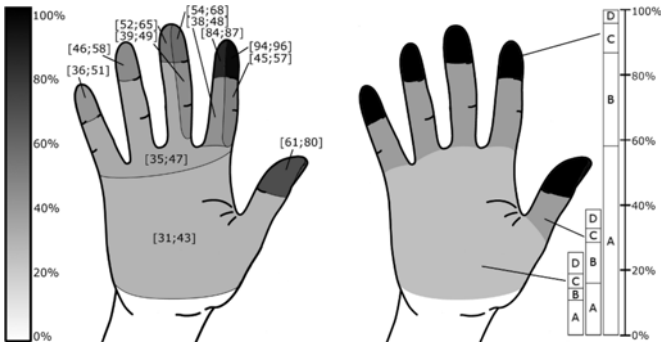

Fig. 7. General map of SIAs and their frequency of use, compared with the percentages of the maximal cumulated densities of the four afferent units : FA I (A), SA I (B), FA II (C), SA II (D) (from [14]).

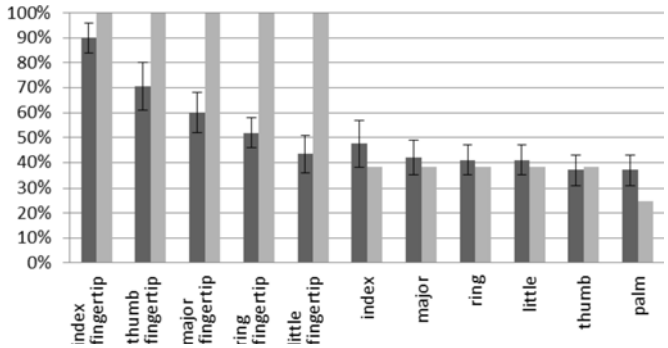

Fig. 8. Correlations between the percentages of use of the hand areas (dark grey, with min and max indicators) and mechanoreceptors (light grey). For light grey bars, 100 percent corresponds to the maximum density of mechanoreceptors over the areas.

and play a key role in tactile sensing through skin deformation and feedback control.

C) FA II (fast adapting type II) afferents end in Pacinian corpuscles, deeper located in the dermis and specialized in the detection of vibrations and transient stimulation. They are very important for the detection of remote events like information from hand-held tools.

D) SA II (slowly adapting type II) afferents stop in Ruffini endings which may play a role in the perception of the movement of an object, and in the sense of weight. They are sensible to skin stretch.

Fig. 7 shows the general map of the simplified interaction areas (left) along with the cumulated densities of the four afferents in the glabrous skin (right). In the latter, the fingertips appear to have more than twice the density of mechanoreceptors as much as the rest of the hand, and more than 70 percent of these are FA I and SA I units which respond to skin deformation and static force. The rest of the fingers is 50 percent less dense, and the palm comes last. This can be taken as a basis to build a map of the areas for which it is important to maintain the mechanoreceptors in a healthy state, as pointed out by Tubiana [15].

The frequencies of use highlight a good matching with the densities of mechanoreceptors (Fig. 8). The fingertips are the most densely populated and the most frequently used, then comes the metacarpus and finally the palm. However, some outliers appear. The most important one is that the fingertips are almost of the same density of mechanoreceptors, whereas the frequency of use decreases from the index to the little. This may be explained by an increasing use of the fingers closer to the thumb, due to mechanical and comfort considerations.

3 Analysis of Hand Interaction Capabilities: Building a Hand Interaction Tree

The above interaction maps give some cues on the contact areas of interest. They provide an insight on the way the hand areas are usually solicited, but not on which activities can be performed depending on the involved contact surfaces.

3.1 General Hand Interaction Tree

To solve this issue, we first assigned some potential *efficiency ranges* to the 24 contact surfaces of Figs. 2 and 4 (M_1 to M_{21} and E_1 to E_4 with $M_{21} = E_4$), corresponding to the sum of the frequencies of use of the interactions they allow respectively:

- For the contact surfaces which do not encompass any other, these ranges are directly calculated as the lower and upper bounds of the weighted sum of data from Figs. 2 and 4, assuming that an average behavior is obtained from the variation of weights from 25 to 50 percent for each profile (i.e., rough manipulation = housemaid, precise manipulation = machinist, and exploration). As an example, the bounds of the *efficiency range* of the contact surface M_2 are equal to:

$$LB_{M_2} = \min(W_m T_{\%M_2 m} + W_h T_{\%M_2 h} + W_e T_{\%M_2 e}) \quad (4)$$

$$UB_{M_2} = \max(W_m T_{\%M_2 m} + W_h T_{\%M_2 h} + W_e T_{\%M_2 e}), \quad (5)$$

  with W_m, W_h and W_e the weights of the machinist, housemaid and exploration data respectively (each one ranging from 0.25 to 0.5) and $T_{\%M_2 m}$ the percentage of time M_2 is used by a machinist (18.8 percent), $T_{\%M_2 h}$ the amount of time it is used by a housemaid (11.6 percent) and $T_{\%M_2 e}$ its frequency of use for exploration (0 percent). We obtain

$$\begin{aligned} LB_{M_2} &= 0.25 T_{\%M_2 m} + 0.25 T_{\%M_2 h} + 0.5 T_{\%M_2 e} \\ &= 0.25 \times 18.8 + 0.25 \times 11.6 + 0.5 \times 0 = 7.6\% \\ UB_{M_2} &= 0.5 T_{\%M_2 m} + 0.25 T_{\%M_2 h} + 0.25 T_{\%M_2 e} \\ &= 0.5 \times 18.8 + 0.25 \times 11.6 + 0.25 \times 0 = 12.3\%. \end{aligned}$$

- The *efficiency range* of a contact surface which encompasses some others is the sum of the ranges of these surfaces. For example, the *efficiency range* of M_5 is the sum of the ranges of use of surfaces E_1, E_2, M_3, M_4 and M_5, i.e., with respect to Figs. 2 and 4: $[15.5; 31] + [3.6; 7.2] + [2.2; 3.4] + [4.7; 8.4] + [2.7; 4.6] = [28.7;\ 54.5$ percent$]$ (rounded values).

These *efficiency ranges* give an estimation of the time during which each contact surface may allow a natural interaction with the environment.

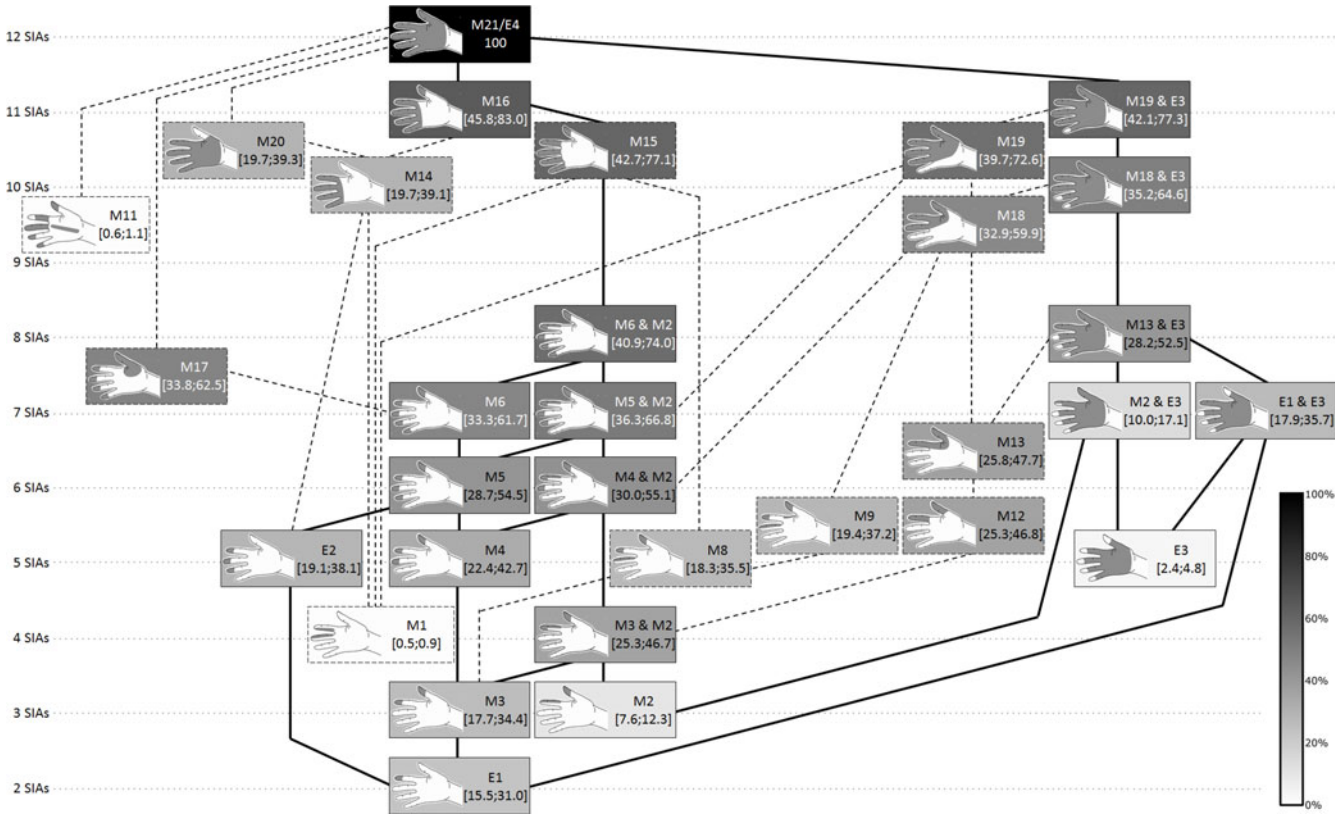

Fig. 9. A hand interaction tree of the contact surfaces and their combinations as a function of the number of their SIAs and the time (displayed in gray-scale and percent) they allow to interact naturally with the environment.

It is worth noting that manual interactions cannot only occur with one of the 24 canonical surfaces from Figs. 2 and 4 but also with any conceivable hand surface. Therefore the *efficiency range* is also computed for some of their combinations. In order to restrain the complexity of the results, only the combinations which significantly increase their *efficiency range* are considered. These combined surfaces are labelled according to their constitutive basic areas (e.g., M_3 and M_2).

From this data, a hand interaction tree is generated (Fig. 9). All canonical contact surfaces are first organized vertically as a function of the number of SIAs they are composed of. For example, the contact surface M_5 is composed of 6 SIAs (thumb, left and right side of index, left and right side of middle, and ring fingertips, see Fig. 6). So it is located above the hand contact surfaces composed of 5 or less SIAs and below those of 7 SIAs or more. If the palm or metacarpus is partly involved, it is accounted for 1/2 SIA (e.g., M_{11}).

In a second step, these areas are connected, considering that two surfaces are linked if the upper encompasses the lower. Some multiple links appear if a given surface is part of several others. However, redundant links are avoided: for example, M_{17} includes E_2 but no link connects them as E_2 is already taken into account through M_5 and M_6.

Some contact surfaces are rarely used and therefore considered as being less interesting as they give access to a very little amount of supplementary natural interaction while being composed of more SIAs (e.g., M_8 counts 5 SIAs and allows interacting naturally with the environment 18.3 to 35.5 percent of the time, i.e., only 0.6 to 1.1 percent more than M_3 for 2 extra SIAs). They are displayed with dotted links.

This tree illustrates the general complexity and efficiency of the various hand contact surfaces in a synthetic way. A critical path (composed of the fingertips and index's lateral side) appears that distinguishes, in function of the number of SIAs, the surfaces to be taken into account to grant access to the most utilized patterns over time. It is worth noting that the ranges of use of the contact surfaces that belong to this critical path are close to those of more conventional areas including the fingertips exclusively. For a given number of SIAs, a focus on a contact surface instead of the other may therefore depend on the specificities of the activity being performed and its influence on the frequencies of use of the various contact surfaces. However, the lateral surface of the index is once again highlighted as it provides a valuable alternative to the consideration of the fingertips only.

The tree is thought to provide a graphical tool to help in the choice of the areas to focus on, for example in the building of a haptic interface. Besides, an available indirect approach to determine the amount of interactions which access is granted by the various parts of the hand is to examine the impairments induced by amputations. Indeed, an amputation of a part of the hand results in that any pattern connected to the associated hand surface cannot be performed any more. The next section compares the interaction tree with its amputation-induced counterpart.

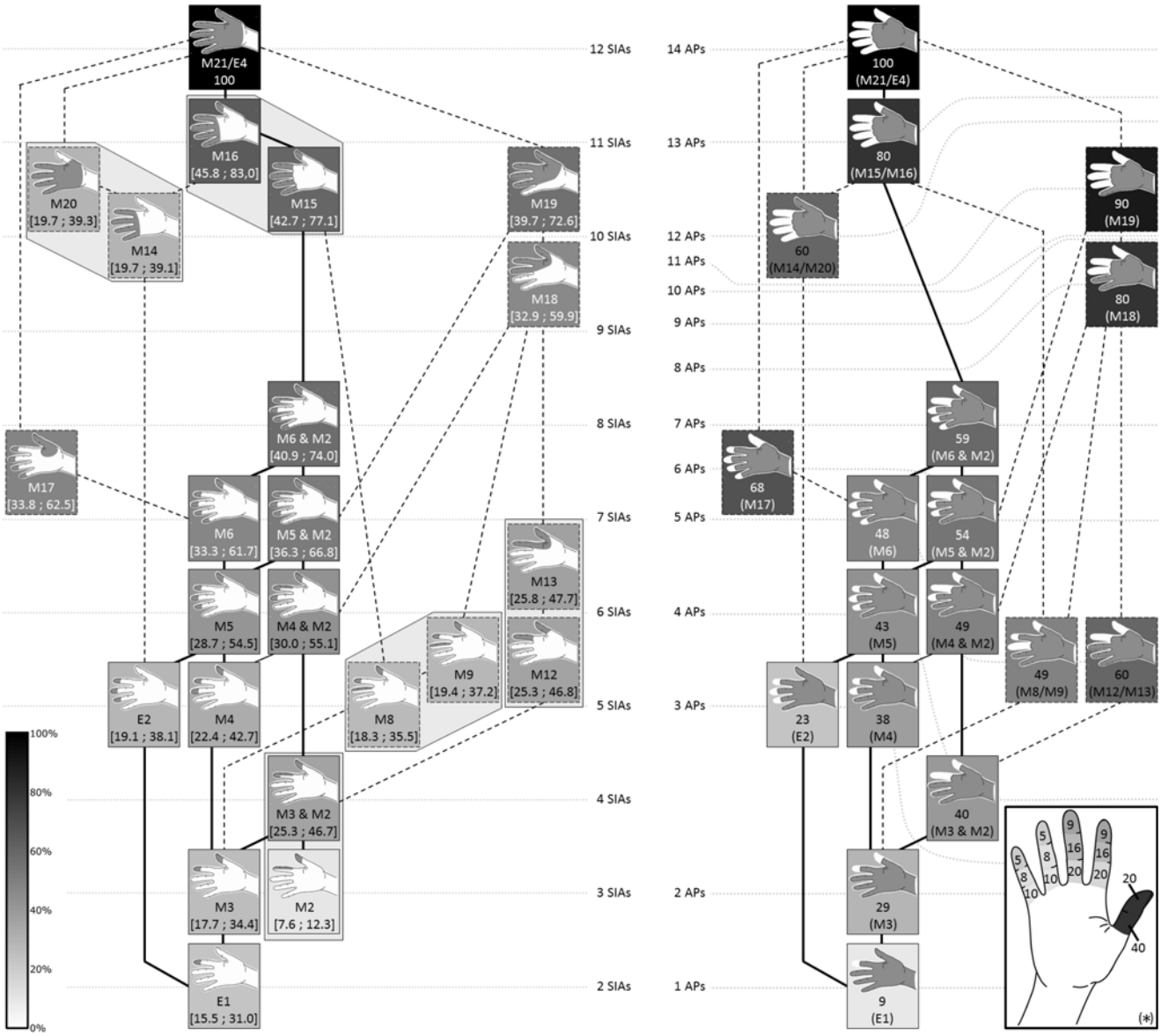

Fig. 10. A comparison of the interaction tree (left) with an impairment tree (right, compiled from the impairment rating map $(*)$ [16], [17]. The amputated areas are in white): the figures and grayscale represent the percentages of loss of hand function in case of amputation at the corresponding joint, e.g., an amputation of the ring fingertip would result in a 5 percent loss of function of the hand, whereas the amputation of the whole thumb is associated with a 40 percent loss of function. APs: Amputated Phalanges.

3.2 Hand Impairments

The ratings devised by Swanson [16] can provide an image of the percentages of loss of hand capability as a function of the amputated phalanges, i.e., they show how useful the amputated areas are, and thus mirror the *efficiency indexes* of the interaction tree.

In this sense, Fig. 10 maps the interaction ability tree (left) to its amputation-induced inability tree counterpart designed using data from [17] and [16] (right). The latter renders the inclusions of amputated areas through the links between the corresponding amputated hands. One can note that some of the skin areas do not involve the fingertips (e.g., E_3 and above) and therefore have no amputated equivalent as it would make no sense to consider that they could remain isolated from the hand. So these surfaces are not considered, as well as very specific ones (e.g., M_1, M_{11}). Also, some contact surfaces correspond to the same amputated areas (e.g., M_2 and above) and cannot be distinguished in the amputation tree. Others differ only by the involved palm surface (i.e., M_8 and M_9, M_{12} and M_{13}, M_{14} and M_{20}, M_{15} and M_{16}). Such surfaces are similar in regard of impairments because the palm is not considered for amputations, so they are grouped in one equivalent amputated hand. The amputated areas are organized vertically as a function of the number of missing phalanges, which gives an idea of the complexity of the lost hand surface. One can note that the vertical scales of the left and right trees differ from each other.

A look at both trees shows an overall good correlation between the interaction capabilities offered by a given hand surface and the inabilities induced by the loss of the same area, confirmed by a closer analysis (Fig. 11). However, some exceptions appear: first, the index distal phalanx has a smaller impact for amputations and involves a

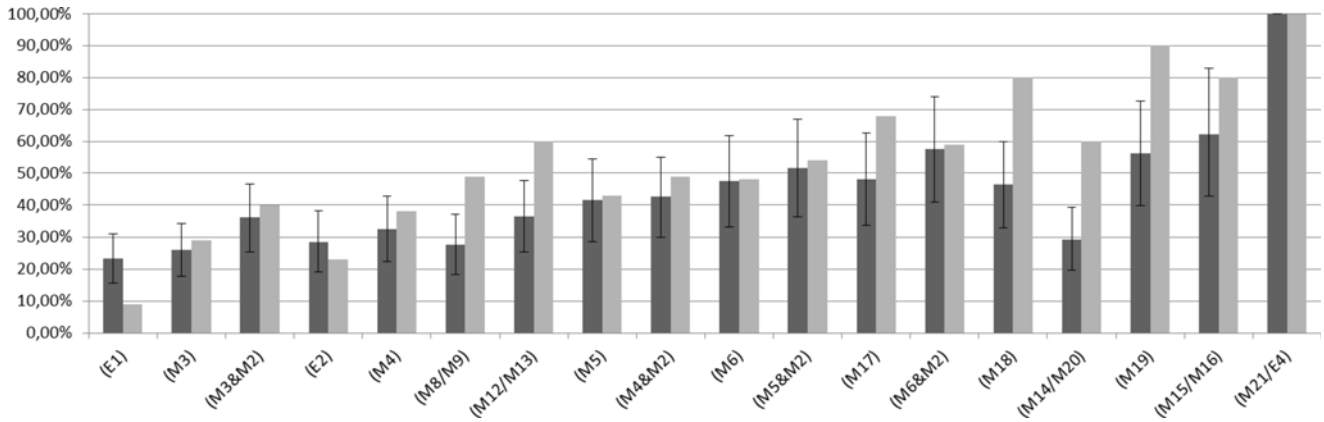

Fig. 11. Correlations with amputations (in percent). Dark grey: contact areas with min and max indicators; light grey: amputations.

decorrelation on (E_1). This is probably due to the large influence of the index fingertip for exploration procedures (especially for contour following) which is less critical for impairments, as the same function can be performed with another finger. Second, the thumb has a greater importance according to the impairment rating. This induces an overrating that propagates through (M_8/M_9), (M_{12}/M_{13}), (M_{18}) and (M_{19}). Finally, the rating of all the fingers induces a difference in (M_{14}/M_{20}). This decorrelation may be due to adaptation, as the thumb alone may be more easily used to grasp objects between thumb and palm than any other finger. Despite its precision as regards the differences in the loss of hand function among the phalanges, the influence of an amputation may vary according to the activity usually being performed by the amputated worker.

The examination of the hand impairments matches the results of the above ergonomic approach as the thumb is the most needed, then the fingertips of the index and middle, finally the fingertips of the ring and the little. However, because the limits of our contact surfaces do not always follow the joints of the hand, our approach is further detailed.

4 Application to the Rating of Haptic Interface Capabilities

The definition of the specifications for choosing or building a generic haptic interface in response to any set of tasks can be challenging [18]. The observation of the involved contact surfaces through the tree built in previous section can be seen as a supplementary tool amongst other criteria to help in this choice, as demonstrated in the sequel.

4.1 Performance Criteria

A perfect generic dexterous haptic interface is expected to simulate efficiently every interaction between an operator and the environment. This would require the interface to render a contact with a variable geometry while providing force feedback in accordance with human limits in perception and action, similar bandwidths and full workspace. In practice, dexterous haptic interfaces do have limits so they rather try to focus on expected performances in specific simulation situations (see examples in Section 1), where speeds and efforts are limited to less extreme values. In this paper, we focused on a general interaction situation. In this context, we propose to use the following criteria to rate dexterous haptic interfaces:

- The *maximum (theoretical) efficiency index* (EI_{max}) is defined as the percentage of time during which the hand surfaces in contact with the end effectors of the interface allow to interact naturally with the environment. It is a measurement of the interface's ability to simulate efficiently the behavior of any virtual object, provided that it is perfectly transparent. It is computed here as the mean of the percentages of the involved contact surfaces, taken from the interaction tree relevant to the considered general set of tasks.
- The *controlled DOFs index* (I_{DOF}) is the ratio between the interface's DOFs with force feedback per SIA and the ones required to interact naturally with the environment. It is first computed for each couple of interface's end effector and corresponding SIA. Then the global I_{DOF} is obtained from a mean of these values. Our hypothesis is that applying 3 forces (1 normal and 2 tangential) on a fingertip is sufficient for a good rendering. On the palm, the display of 3 forces and 3 torques is required. It is worth noting that rendering a normal force on every surface involved in a particular grasp can appear sufficient to simulate the grasping of the associated objects. However, the objects' weights also produce tangential forces on the areas which are not normal to gravity (and torques for large ones). Similarly, when an object (especially a tool) interacts with the environment, tangential forces are generated at the skin surface. Consequently, 3D forces (respectively 6D efforts for large areas) are required to efficiently simulate remote or virtual manipulation. One can note that the DOFs can be weighted. For example, in order to take the prevalence of grasping into account in this paper, we counted 50 percent for a normal force in order to emphasize its control, and 25 percent per tangent direction.
- The *workspace index* (I_{WS}) is calculated as the mean percentage of the human workspace spanned by each end-effector of the interface. For wearable and portable devices which can freely follow the movements of the hands, only the movements of the fingertips with respect to the palm are taken

into account. Conversely, for fixed devices which globally limit the movements of the hand, both the workspaces of the fingers and the hand are considered and multiplied. For most interfaces, the percentage of the fingers' workspace which is spanned by the interface can be easily retrieved from the literature. There is no such information for the arm, so we decided to rely on ergonomic standards and gave an interface a score of 100 percent if it can move over the full arm's workspace, 75 percent if it can move over the acceptable volume (about $1{,}500 \times 500 \times 500$ mm in front of the user), 50 percent if it can span the comfortable volume ($1{,}100 \times 300 \times 300$ mm) and 25 percent if the hand can barely move [19].

- The *force capability index* (I_F) is defined as the ratio of the interface's maximum force capability over the force required to efficiently simulate contacts with virtual objects. Most dexterous interfaces are of the same force capability for all contact areas in all directions. If not, a mean value is computed. The required force differs across users and depends on the grasp type, arm configuration and force direction [20]. Maximum forces range from about 50 N to more than 120 N for precision grasps and from less than 150 N to more than 500 N for power grasps, but in practice, considering 40 N for the palm and 10 N for the fingers as the highest required peak forces seems reasonable since they allow to perform up to 90 percent of daily activities [17] and larger forces cannot be applied for a long time [20].
- The *stiffness index* (I_K) is the ratio of the maximum stiffness of an interface over the one required to render realistic contacts against stiff objects. Since the mechanical stiffness of a haptic interface is rarely given in its specifications, we chose to assimilate it to the stability limitations on its control gains. A stiffness of 24,200 N/m is theoretically required to simulate a hard wall based on haptic feedback only [21], but combined to visual feedback, a compelling illusion of hardness is obtained at about 5,000 N/m. This value is used here as a target.

Finally, a global efficiency index can be computed by multiplying all these criteria, so as to assign a rate to an interface as an expression of its effectiveness in regard of a set of tasks to simulate.

4.2 A Review of Some Dexterous Haptic Interfaces

In this section, some generic dexterous haptic interfaces are rated according to the aforementioned criteria. They are representative of the diversity of the devices which can be found on the market and in laboratories. For each interface, a radar diagram displays the value of each criterion involved in the calculus of the global interaction efficiency, which is displayed in grayscale below it (Fig. 12):

a) The PERCRO PHFE is a thumb-index-fingertip interface [22] allowing to interact through M_3 (so $EI_{max} = 26.1\%$). It is composed of two six-DOF robots with three motors each, controlling three DOFs for each fingertip, thus $I_{DOF} = 100\%$. Both robots are attached to a base worn on the forearm. Each robot spans the whole workspace of the corresponding finger. However, the fingertips are attached to the end-effectors with large thimbles which prevent them from being close to each other. This limit is included by decreasing the workspace index to $I_{WS} = 90\%$. Its force capability is above 4 N continuous and 25 N peak and its stiffness larger than 5,900 N/m. That exceeds the required limits ($I_F = I_K = 100\%$). Consequently, the interaction efficiency equals 23.5 percent.

b) The IHS10 glove [23] is a three-fingertip device which grants access to every interaction involving M_4 ($EI_{max} = 32.6\%$). It is composed of three five-DOF robots with three motors each, allowing for three DOF per fingertip to be controlled ($I_{DOF} = 100\%$). As well as for the PHFE, its workspace spans the one of the fingers but the thimbles prevent them

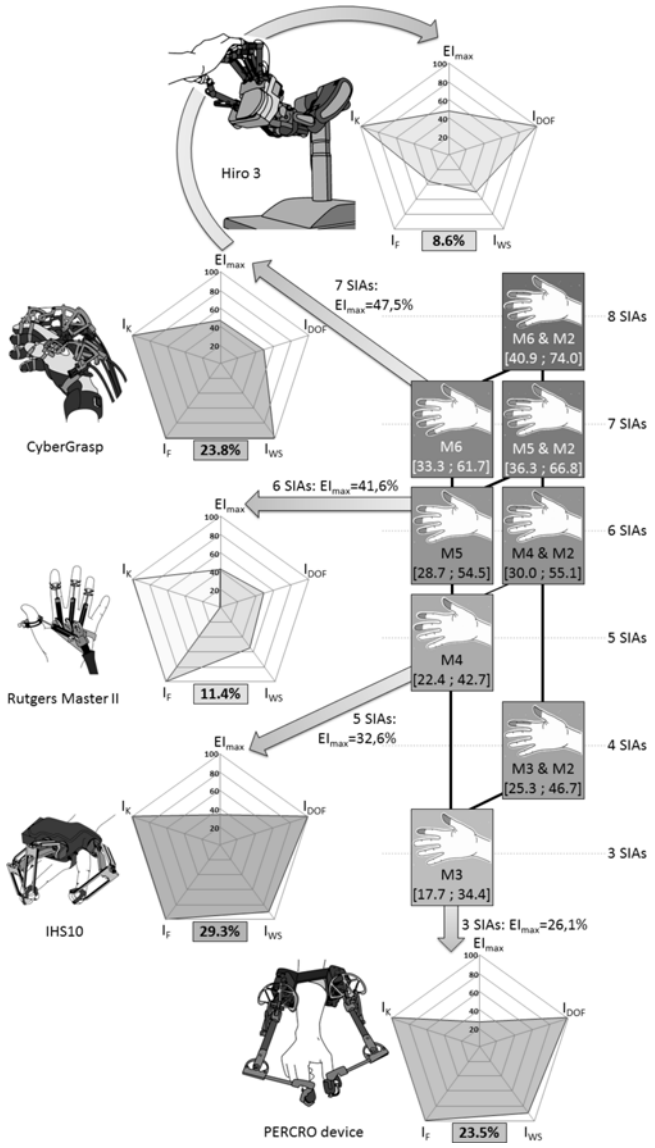

Fig. 12. A demonstration of the use of the interaction tree for the rating of existing haptic interfaces (all values in percent). EI_{max}: maximum efficiency index; I_{DOF}: controlled DOFs index; I_{WS}: workspace index; I_F: force capability index; I_K: stiffness index. The grayscale numbers under the radars are the resulting global efficiency indexes.

from being close to each other, thus I_{WS} is set at 90 percent. Its peak force capability and control stiffness are higher than 10 N and 5,000 N/m respectively, thus $I_F = I_K = 100\%$. Its interaction efficiency equals 29.3 percent.

c) The Rutgers Master II [24] is a four-fingertip haptic interface allowing to interact through M_5 ($EI_{max} = 41.6\%$). Force feedback is provided by air cylinders located inside the palm and is only available along the normal to each contact surface. This corresponds to $I_{DOF} = 50\%$. Besides, this technology limits the hand closure to 55 percent of natural grasping motion as the air cylinders have a minimum dimension approaching half their maximum size, thus $I_{WS} = 55\%$. The maximum force feedback is above 16 N and the maximum control stiffness is about 8,000 N/m (data from private discussions with the Rutgers Master II designer), therefore $I_F = I_K = 100\%$. As a whole, the interaction efficiency of this device is 11.4 percent.

d) The Cybergrasp is a five-fingered dexterous haptic glove. Its mechanical structure is a semi-exoskeleton allowing for coupled force feedback on the fingertips and middle phalanges. Therefore, we considered it as a fingertip device giving access to interactions associated with M_6 ($EI_{max} = 47.5\%$). I_{DOF} is limited to 50 percent as its actuators allow force feedback along the normal to the fingertips only. Free finger movements are permitted (i.e., $I_{WS} = 100\%$), as it is lightly connected to the fingertips. Its force capability is 12 N and its control stiffness can be set up to 50,000 N/m [25] so $I_F = I_K = 100\%$. We finally obtain an interaction efficiency of 23.8 percent.

One could argue that this system is not a real fingertip device since it allows interactions with medial phalanges, i.e., a combination of M_{15} and M_{12}. This would greatly increase EI_{max}. However, in this case, it would be fair to consider that I_{DOF} is divided by 2 as the feedback is coupled on the medial and distal phalanges. As a whole, the interaction efficiency would be similar, if not lower.

e) The HIRO III arm [26] is a five-fingertip opposed-type haptic interface allowing to interact through M_6 ($EI_{max} = 47.5\%$). It allows force feedback in three DOF for each fingertip ($I_{DOF} = 100\%$). Contrary to previous interfaces, it is a fixed robot. Consequently, although it can span the fingers' workspace, the hand movements are limited to half a torus which largest dimensions are about $740 \times 370 \times 370$ mm, approaching the comfortable working volume of the hand, so $I_{WS} = 100 \times 50 = 50\%$. Its force capability is only 3.6 N at the fingertips while its maximum stable control stiffness exceeds 5,000 N/m. Thus $I_F = 36\%$ while $I_K = 100\%$. Hence an interaction efficiency of only 8.6 percent.

As a synthesis of this review, Fig. 13 displays the interaction efficiencies of the interfaces and the maximum efficiency indexes of the associated interaction areas as a function of their number of SIAs. It highlights that relatively simple interfaces like the IHS10 glove can be of a higher interaction efficiency than more complex ones like the CyberGrasp or Hiro III device. This result suggests that it would be of interest to do research on articulation technologies, actuation and control to approach 100 percent simultaneously for I_{DOF}, I_F and I_K, even for complex architectures.

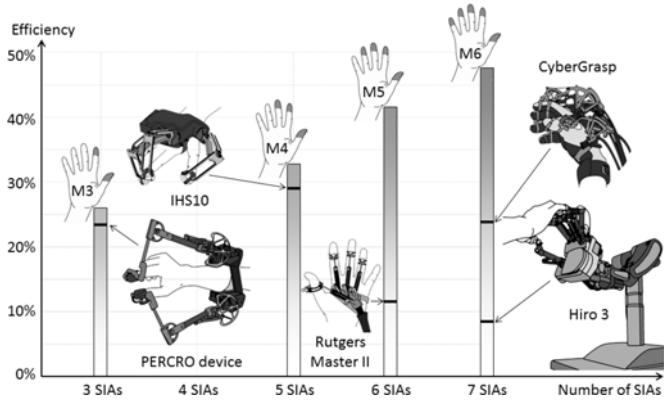

Fig. 13. Interaction efficiency of some existing interfaces (black dashes, percent) and maximum efficiency indexes of the associated interaction areas (bars, percent) as a function of their number of SIAs.

One can note that these results may be optimistic: the mechanical stiffness along with the control one probably decreases the stiffness felt by the user. Also, other criteria can be added, like friction or bulkiness. The influence of the latter would depend on the virtual reality setup (e.g., none with a head-mounted display), so it was not taken into account in this paper. However, the drawings of the devices in Fig. 12 are on the same scale, so that their bulkiness can be noticed.

4.3 Design Guidelines for Haptic Interfaces

The ratings of previous paragraph are valuable for a general set of tasks, and therefore apply to devices intended to efficiently simulate any kind of interaction. For such generic designs, Fig. 12 suggests to investigate some new kinematics allowing to track and apply force feedback on the five fingertips and lateral index's surface (M_6 and M_2). Such structures would allow simulating natural interactions which occur almost 60 percent of the time within a virtual environment (considering the mean of the extreme values given in the interaction tree as EI_{max}).

One can also be interested in developing an interface adapted to a particular set of tasks. To help solving this issue, Fig. 14 displays separate interaction trees corresponding to the three stereotypical situations presented in Section 2, with frequencies of use displayed both in figures and grayscale. As explained before, their combination with adequate weights grants access to any set of tasks balanced between fine and rough manipulation and exploration.

However, one can note that these stereotyped trees are of interest by themselves since they account for the design of specific haptic interfaces. For example:

- The interaction tree of the machinist, whose interactions are predominantly fine manipulation tasks, is well suited to guide the design of an interface dedicated to simulating fine assembly activities. It

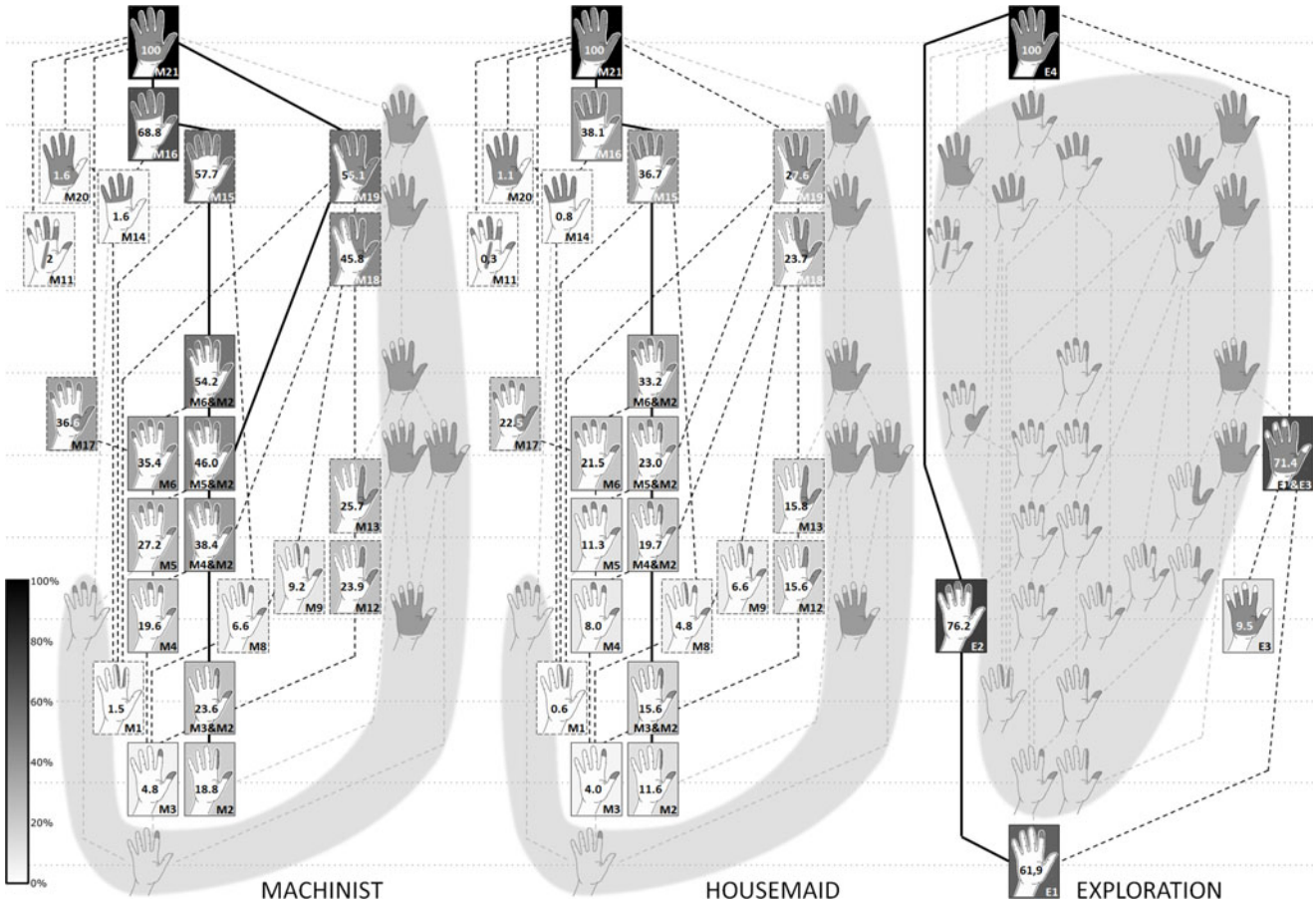

Fig. 14. Interaction trees corresponding to three stereotypical sets of tasks (fine manipulation: machinist, rough manipulation: housemaid, exploration). The frequencies of use of the different interaction areas are displayed both in grayscale and figures. The grey areas correspond to the unused parts of the general interaction tree.

features a slightly different critical path compared to Fig. 9 as it emphasizes even more the index's lateral surface. This suggests the development of a haptic interface focused on this area and the five fingertips since it would grant access to more than 50 percent of the corresponding interactions.

- The interaction tree of the housemaid is representative of rough manipulation tasks. In this case the critical path is similar. However, addressing all fingers does not allow a natural interaction for more than 40 percent of the time, whereas the addition of the palm drastically increases this figure. This suggests that a device equipped with a handle is well suited for such tasks, although it does not allow to track and render forces on each finger.
- Finally, the critical path is different in case of an exploratory task. The use of the index's fingertip grants access to most of the exploratory patterns, so a vibrotactile haptic interface adapted to this sole area can be sufficient for pure exploration tasks. Although more complex, haptic feedback on the index, middle and ring fingers appears as a must in this case.

5 Conclusions

This article develops some methodologies used to build graphical tools allowing to study hand interactions. The goal is to help in the design of dexterous haptic interfaces. The proposed tools consist in an interaction map and an interaction tree.

From the frequencies of use of grasp and exploratory patterns, three different interaction maps have been set up: one for exploration tasks and two for both rough and fine manipulation. A weighted map is then built as a combination of the three maps and is intended to reflect the relative importance of the various hand areas during an average manual task, i.e., involving fine and rough manipulation along with exploration activities. It highlights the importance of the fingertips for manual interactions. The thumb and the index fingertips are the most important, then comes the middle's, finally the ring's and the little's. The lateral surface of the index and the fingertip of the ring are used with an equal frequency: this finding may allow to consider the design of haptic interfaces addressing the lateral area of the index rather than the ring. The remaining fingers' areas and the palm are less used during manual tasks.

Then, various associations of the defined hand contact areas are examined in order to enhance the interaction capabilities while keeping the number of associated areas as small as possible. This ultimately consists in choosing the hand contact areas that a dexterous haptic interface should address to increase the operator's telepresence without making its design too complex. A graphical interaction tree

is built to ease the analysis. As an illustration of its interest, a ranking of some existing dexterous haptic interfaces is achieved, which takes into account interaction efficiency. It is also used to suggest guidelines for the design of haptic interfaces featuring a good ratio between interaction capabilities and complexity, considering both generic and specific interactions.

The two main results, i.e., the most frequently used hand areas and the interaction capabilities as a function of the association of various hand areas, are correlated to other findings available in the literature. First, it appears that the most frequently used hand areas enclose the highest density of mechanoreceptors. Second, the interaction tree which illustrates the interaction efficiency as a function of the number of utilized hand areas is correlated to the decrease of the interaction quality, induced by phalanges amputation.

The analysis presented in this paper can be strengthened by considering a larger set of possible manual interactions. For example, further data recording is expected to better highlight the role of the palm for gesture stabilization during fine manipulation, since precise movements (e.g., miniature objects assembly) may require the proximal part of the palm to be rested on a stable surface while the fingers are performing the task. Considering bimanual interactions would be of interest as well in order to better understand the way the hand is used. Model-based tracking techniques [27] handling occlusions might make data recording easier. Meanwhile, the developed methods are generic enough to be applied on any new data.

The present work is aimed to help in the design of efficient and simplified dexterous haptic interfaces through the analysis of the most frequently hand areas. It is complementary to the research presented in [28] where the authors analyzed the most frequently grasp patterns to help reducing the complexity of prosthetic and robotized hands. These two studies may be further deepened by considering the results of [20], [29] where the grasping forces and the hand synergies are studied.

Acknowledgments

The authors wish to thank Professor Vincent Hayward for his valuable advice and comments during this research. Part of this work has been published in the *Proceedings of the IEEE WHC'13*. This research was partly supported by the "Agence Nationale de la Recherche" (Mandarin project - ANR-12-CORD-0011, labeled by "Cap Digital Paris Région," the French cluster for digital contents and services), and partly accomplished within the laboratory of excellence SMART supported by French state funds managed by the ANR within the Investissements d'Avenir program (ANR-11-IDEX-0004-02).

References

[1] K. Shimoga, "A survey of perceptual feedback issues in dexterous telemanipulation: Part 1. Finger force feedback," in *Proc. Int. Symp. Virtual Reality*, 1993, pp. 271–279.

[2] S. P. Christodoulou, D. M. Garyfallidou, G. S. Ioannidis, and T. S. Papatheodorou, "Interactive education based on haptic technologies and educational testing of an innovative system," in *Int. J. Emerging Technologies in Learning*, vol. 3, no. 2, pp. 4–19, 2008.

[3] G. Trannoy, J. Lozada, and C. Mégard, "IHS10, Etude des interactions conducteur commandes véhicule d'une voiture Peugeot 308," CEA, Noisy-Le-Grand, France, Tech. Rep. DTSI/SRCI/08-522, 2008.

[4] Y. Yokokohji, N. Muramori, Y. Sato, and T. Yoshikawa, "Designing an encountered-type haptic display for multiple fingertip contacts based on the observation of human grasping behavior," in *Proc. IEEE Int. Symp. Haptic Interfaces Virtual Environ. Teleoperator Syst.*, 2004, pp. 66–73.

[5] M. Cutkosky, "On grasp choice, grasp models, and the design of hands for manufacturing tasks," *IEEE Trans. Robot. Autom.*, vol. 5, no. 3, pp. 269–279, Jun. 1989.

[6] T. Feix, R. Pawlik, H. Schmiedmayer, X. Romero, and D. Kragić, "A comprehensive grasp taxonomy," in *Proc. Robot., Sci. Syst. Conf.: Workshop Understanding Human Hand Adv. Robot. Manipulation*, 2009, available at grasp.xief.net.

[7] L. Jones and S. Lederman, *Human Hand Function*. Oxford, NY, USA: Oxford Univ. Press, 2006.

[8] J. Zheng, S. De La Rosa, and A. Dollar, "An investigation of grasp type and frequency in daily household and machine shop tasks," in *Proc. IEEE Int. Conf. Robot. Autom.*, 2011, pp. 4169–4175.

[9] C. Taylor and R. Schwartz, "The anatomy and mechanics of the human hand," *Artif. Limbs*, vol. 2, no. 2, pp. 22–35, 1955.

[10] J. Napier, "The prehensile movements of the human hand," *J. Bone Joint Surg.*, vol. 38B, pp. 902–913, 1956.

[11] N. Kamakura, M. Matsuo, M. Ishii, F. Mituboshi, and Y. Miura, "Patterns of static prehension in normal hands," *Ame. J. Occupa. Therapy*, vol. 34, pp. 437–445, 1980.

[12] I. M. Bullock, R. R. Ma, and A. M. Dollar, "A hand-centric classification of human and robot dexterous manipulation," *IEEE Trans. Haptics*, vol. 6, no. 2, pp. 129–144, Apr.-Jun. 2013.

[13] S. Lederman and R. Klatzky, "Haptic perception: A tutorial," *Attention, Percept. Psychophys.*, vol. 71, no. 7, pp. 1439–1459, 2009.

[14] A. Vallbo and R. Johansson, "Properties of cutaneous mechanoreceptors in the human hand related to touch sensation," *Human Neurobiol.*, vol. 3, pp. 3–14, 1984.

[15] R. Tubiana, "Architecture, functions of the hand," in *Examination of the Hand and Upper Limb*, Philadelphia, PA, USA: Saunders, 1984.

[16] A. Swanson, "Evaluation of impairment of function in the hand," *Surg. Clinics North Amer.*, vol. 44, pp. 925–940, 1964.

[17] L. Jones, "Dextrous hands: Human, prosthetic, and robotic," *Presence*, vol. 6, no. 1, pp. 29–56, 1997.

[18] E. Samur, *Performance Metrics for Haptic Interfaces*. New York, NY, USA: Springer-Verlag, 2012.

[19] *Postures et dimensions pour l'homme au travail sur machines et appareils*, French Standards Assoc., NF X35-104, vol. 10, 1983.

[20] B. Daams, *Human Force Exertion in User-Product Interaction—Background for Design*. Amsterdam, the Netherlands: Delft Univ. Press, 1994.

[21] H. Z. Tan, M. A.Srinivasan, B. Eberman, and B. Cheng, "Human factors for the design of force-reflecting haptic interfaces," *Dynam. Syst. Control*, vol. 55-1, pp. 353–359, 1994.

[22] A. Frisoli, F. Simoncini, M. Bergamasco, and F. Salsedo, "Kinematic design of a two contact points haptic interface for the thumb and index fingers of the hand," *ASME J. Mech. Des.*, vol. 129, no. 5, pp. 520–529, 2007.

[23] F. Gosselin, "Guidelines for the design of multi-finger haptic interfaces for the hand," in *Proc. 19th CISM-IFToMM Symp. Robot Des., Dynam. Control*, 2012, pp. 167–174.

[24] M. Bouzit, G. Burdea, G. Popescu, and R. Boian, "The Rutgers master II—New design force-feedback glove," *IEEE/ASME Trans. Mechatronics*, vol. 7, no. 2, pp. 256–263, Jun. 2002.

[25] M. Aiple and A. Schiele, "Pushing the limits of the CyberGrasp™ for haptic rendering," in *Proc. IEEE Int. Conf. Robot. Autom.*, 2013, pp. 3541–3546.

[26] T. Endo, H. Kawasaki, T. Mouri, Y. Ishigure, H. Shimomura, M. Matsamura, and K. Koketsu, "Five-fingered haptic interface robot: HIRO III," *IEEE Trans. Haptics*, vol. 4, no. 1, pp. 14–27, Jan./Feb. 2011.

[27] I. Oikonomidis, N. Kyziazis, and A. Argyros, "Full DOF tracking of a hand interacting with an object by modelling occlusions and physical constraints," in *Proc. IEEE Int. Conf. Comput. Vis.*, 2011, pp. 2088–2095.

[28] I. M. Bullock, J. Z. Zheng, S. De La Rosa, C. Guertler, and A. Dollar, "Grasp frequency and usage in daily household and machine shop tasks," *IEEE Trans. Haptics*, vol. 6, no. 13, pp. 296–308, Jul.-Sep. 2013.
[29] M. Santello, M. Flanders, and J. F. Soechting, "Postural hand synergies for tool use," *J. Neurosci.*, vol. 18, no. 23, pp. 10105–10115, 1998.

Franck Gonzalez received the Ing degree from the Arts et Métiers Paristech, Paris, and the MSc degree in robotics and advanced systems from the Université Pierre et Marie Curie (UPMC) in 2011. He joined the Interactive Robotics Laboratory at CEA-LIST Institute in 2012, where he is working toward the PhD degree in mechatronics. His research interests include haptic device design, force-feedback displays, and robotics. He is a student member of the IEEE.

Florian Gosselin received the Ing degree in robotics from the Ecole Centrale de Nantes in 1995 and the PhD degree in mechanical engineering from the University of Poitiers in 2000. He is working as a research engineer and project manager at CEA-LIST Institute, Interactive Robotics Laboratory. His research interests include haptics and robotics. He designed numerous haptic interfaces and took part in their integration in state-of-the-art multimodal VR platforms with applications in CAD, digital mock-up, telesurgery, cultural heritage, digital arts, entertainment, and e-learning.

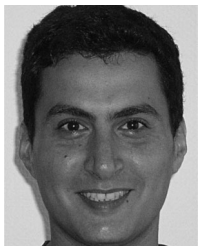

Wael Bachta received the Electr Eng degree from the Ecole Nationale Supérieure de Physique de Strasbourg in 2005, and the MS and PhD degrees in robotics from the University Louis Pasteur, Strasbourg, France, in 2005 and 2008, respectively. He is currently an associate professor at the Université Pierre et Marie Curie—Paris 6, France, where he is a member of the Institut des Systèmes Intelligents et de Robotique (ISIR). His research interests include medical robotics and robot control.